

# Geometric and Simulation Parameter Effects on Elastic Moduli of Multi-Walled Carbon Nanotubes Using Molecular Dynamics Approach

*Hunain Alkhateb<sup>1</sup>, Ahmed Al-Ostaz<sup>1</sup>, Alexander H.-D. Cheng<sup>1</sup> and, P. Raju Mantena<sup>2</sup>*

<sup>1</sup>University of Mississippi, Department of Civil Engineering, University, MS, 38677

<sup>2</sup>University of Mississippi, Department of Mechanical Engineering, University, MS, 38677

## **ABSTRACT:**

The molecular dynamics (MD) approach is used to calculate the equivalent continuum mechanics elastic constants for multi-walled carbon nanotubes. These elastic constants are found to be sensitive to the carbon nanotube geometry (chirality, aspect ratio, number of walls) and the MD simulation conditions (temperature, thermodynamic ensemble, barostat and thermostat algorithms). Our analysis shows that for the NVT (constant number of atoms, constant volume, and constant temperature) thermodynamic ensemble, best results are obtained by combining it with an Anderson thermostat algorithm. For the NPT (constant number of particles, constant pressure, and constant temperature) thermodynamic ensemble, it is recommended to use the Berendsen barostat, coupled with Parrinello thermostat.

**Keywords:** Molecular dynamics simulation, multi-walled carbon nanotube, carbon nanotube, elastic moduli, chirality, thermodynamic ensemble, barostat and thermostat algorithm.

# 1. INTRODUCTION

During the last decade, obtaining the mechanical properties of carbon nanotubes (CNTs), experimentally or theoretically, has been the focus of many researchers of nanomechanics. A wide range of values was obtained, depending on the method used. For example, transmission electron microscope (TEM) was used to obtain Young's modulus of multi-walled carbon nanotubes (MWCNTs) by measuring the mean-square vibrational amplitudes of MWCNTs.<sup>1</sup> This technique resulted in a Young's modulus of the order  $1.8\pm 0.9$  TPa. Other experimental techniques, such as atomic force microscopy (AFM), measured an average Young's modulus of MWCNTs to be  $0.81\pm 0.41$  TPa,<sup>2</sup> about half of the above value.

Parallel to experimental efforts, theoretical models have been used to estimate mechanical properties of MWCNT. These models have some inconsistencies as well. For example, modeling MWCNTs as simple structural element (e.g., bar, beam, or shell) ignores certain MWCNT molecular structural details.<sup>3</sup> Li & Chou<sup>4</sup> accounted for the van der Waal forces between tube layers by introducing a nonlinear truss rod model. The results show that Young's modulus of MWCNTs was in the range of  $1.05\pm 0.05$  TPa.

Alternatively, molecular simulations (molecular mechanics and molecular dynamics) have been used as a tool to model MWCNTs. Batra & Sears<sup>5</sup> used molecular mechanics (MM) to determine double-walled carbon nanotube (DWCNT) structures and to analyze their infinitesimal extensional, torsional, radial expansion/contraction and bending deformations, based on a continuum model. Al-Ostaz *et al.*<sup>6</sup> simulated single-walled carbon nanotubes (SWCNTs) using molecular dynamics (MD) approach. SWCNT's elastic constants for different chiralities were calculated, and the effect of clustering of SWCNTs on their effective properties was evaluated. Zhang *et al.*<sup>7</sup> performed MD simulations on MWCNTs under axial compression to investigate the effects of the number of walls, and their van der Waals (vdW) interaction on buckling behaviors.

Although significant progress has been made in finding the mechanical properties of MWCNT both experimentally and theoretically, in MD simulation, it is often found that the simulated results can be sensitive to the various modeling parameters, such as the methods used to build the CNT atomic structure, the size of the modeled cell (how many periodic cells to include), the algorithms used for averaging, the pressure and temperature conditions during

simulation, and the package used in the MD software, etc. Without paying attention to these simulation conditions, inconsistent results can be obtained. Hence the purpose of this paper is to investigate the effects of the above-mentioned and other modeling conditions on the estimated continuum mechanical properties of MWCNT, and to make recommendations for future modeling efforts.

## 2. MOLECULAR DYNAMICS APPROACH

### 2.1 Carbon Nanotube Chirality

One may consider the CNT structure as a two dimensional graphene sheet rolled along a certain vector direction, which defines the CNT's chirality (Figure 1), into a tube. The resulting tubular structure can be single- or multi-walled, depending on the number of layers of the folded graphene sheets,<sup>8</sup> with diameter as small as 1 nm, and a length that can be a few microns. Chiralities of single- and multi-walled CNTs are generally found in random distributions, as their structural details are strongly determined by the thermal history during the manufacturing process.<sup>8</sup> White *et al.*<sup>9</sup> classified SWCNTs by their wrapping vector notation  $(n, m)$ , which describes each structural layer uniquely. In this paper, this classification is extended to incorporate MWCNTs by the wrapping notation  $((n_1, m_1), (n_2, m_2), \dots, (n_i, m_i))$ , where  $(n_1, m_1)$  describes the innermost tube, and  $i$  refers to the total number of the graphene chiral layers.

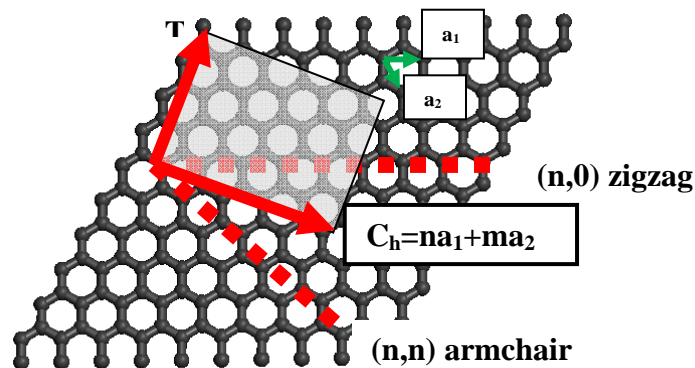


**Figure 1.** The  $(n, m)$  carbon nanotube naming scheme.

## 2.2 Molecular Dynamics Simulation

Molecular dynamics simulate the real dynamics of the CNT system, and are traditionally performed under the conditions of constant number of particles ( $N$ ), volume ( $V$ ), and energy ( $E$ ). It starts by selecting a model system consisting of  $N$  particles. Positions of atoms are determined by applying Newton's equation of motion. The system is simulated until it reaches an equilibrium state, and the elastic properties of the system are determined at that time. MD seeks to determine  $6N$  coordinates and momenta, which are sensitively dependent on the initial conditions. This means that two states with very close initial conditions diverge exponentially through time.<sup>10</sup> As our interest lies only in the equilibrium state, it is important to choose an optimization algorithm that can predict the trajectories of atoms that reach the equilibrium state as quick as possible.

Two approaches are usually used to simulate MD for different thermodynamic ensembles: by mixing Newtonian MD with Monte Carlo technique or by reformulating the Lagrangian equations of motion of the system.<sup>10</sup> Extended Lagrangian method was first introduced by Andersen<sup>11</sup>, in which he discussed MD simulations under constant pressure, constant temperature, or both constant pressure and temperature conditions. The trajectory averages for those three ensembles correspond to the isoenthalpic-isobaric, canonical, and isothermal-isobaric conditions<sup>11</sup> these ensembles have become one of the most important derivations that enabled the improvement of the MD performance. Results obtained from one ensemble could be transformed into another ensemble. These transformations, however, is strictly possible only for a periodic unit cell, which represents an infinite system.

At constant temperature, energy associated with MD simulations fluctuates. A system subjected to a constant temperature is equivalent to maintaining the system in a heat bath. Under such conditions, the dynamic energy follows Boltzmann distribution, and this can be transformed into the following kinetic energy and temperature relation:<sup>10</sup>

$$K_B T = m \langle v_\alpha^2 \rangle \quad (1)$$

where  $m$  is the mass of the particle,  $v_\alpha$  is the ensemble's  $\alpha^{\text{th}}$  velocity component,  $\langle \rangle$  is the average,  $K_B$  is Boltzmann constant and  $T$  is thermodynamic temperature.

On the other hand, at constant pressure, the volume associated with the MD simulation fluctuates. This can be obtained by replacing the coordinates of the particles by scaled coordinates  $\rho_i$ <sup>11</sup>:

$$\rho_i = r_i / \sqrt[3]{V} \quad (2)$$

where  $r_i$ ,  $i=1,2,3,\dots,N$ , are the original coordinates,  $V$  is the volume of unit cell,  $N$  is the number of particles. Each component of  $\rho_i$  is a dimensionless number between (0, 1).

At constant pressure and temperature, the energy, pressure, and enthalpy are fluctuating properties. To be able to calculate the trajectories of such system, a stochastic collision method should be introduced, so that the time average of any function is equal to the Isobaric ensemble average quantity.<sup>11</sup> In this paper, effects of isobaric and isochoric thermodynamic ensemble simulations are studied for MWCNT.

MWCNTs can be simulated as nested SWCNTs. Whereas potential energy interactions in SWCNTs are controlled only by the carbon covalent bonding, the potential energy in MWCNTs is controlled by both covalent and van der Waals forces. It is so far not clear how van der Waals forces affect the elastic constants of MWCNTs. MD can be used to accommodate both covalent and van der Waals effects numerically. MD simulations rely on interaction between molecules and atoms for a period of time under known laws of physics which predicts motion trajectory of particles. This motion depends on assumed forcefield.<sup>12, 13</sup> By ignoring the details of electron – electron and electron- nucleon interactions, the forcefield method works at the atomic level.<sup>14</sup>

### **2.3 MWCNT Simulations**

In order to obtain a good estimation of mechanical properties of MWCNTs, it is important to use correct *geometric* and *simulation* parameters. Geometrical parameters include chirality, number of layers, and aspect ratio. Simulation parameters include heat effect, thermodynamic ensemble, and thermostat and barostat algorithms. The simulated bulk structures maybe subjected to three different methods for evaluating their mechanical behaviors—the static method, the fluctuation method, and the dynamic method. In this paper static method was used.

The commercially available Material Studio Software<sup>®15</sup> is used for performing molecular dynamics simulations of multi-walled carbon nanotube reinforced polymers to predict their mechanical properties. This is accomplished by using bulk amorphous polymer structures generated by constructing polymeric chains in a periodic cell, taking into account the bond torsion probabilities and bulk packing requirements. Crystal structures for semi-crystalline and amorphous polymers are generated.<sup>15</sup> Models are then equilibrated by a series of energy minimization and molecular dynamics runs.

For each configuration submitted for analysis of static elastic constants, the first step consists of energy minimization using conjugate gradients method. Following the initial stage, three tensile and three pure shear strains of magnitude  $\pm 0.0005$  were applied to the energy minimized system, and the system was re-minimized following each deformation.

After MD simulation is performed, the resulting deformed molecular structure is analyzed to determine the elastic constants. Elastic constants of the final atomic configuration are computed using the static approach suggested by Theodorou and Suter.<sup>16</sup> The elastic constants in this approach are defined as<sup>15</sup>:

$$C_{lmnk} = \left. \frac{\partial \sigma_{lm}}{\partial \varepsilon_{nk}} \right|_{T, \varepsilon_{nk}} = \frac{1}{V_o} \left. \frac{\partial^2 A}{\partial \varepsilon_{lm} \partial \varepsilon_{nk}} \right|_{T, \varepsilon_{lm}, \varepsilon_{nk}} \quad (3)$$

In the above,  $A$  denotes the Helmholtz free energy,  $\varepsilon$  is the strain component,  $\sigma$  is the stress component and  $V_o$  is the volume of the simulation cell in the undeformed configuration. It is assumed that contributions originating from changes in configuration entropy on deformation, and from the strain dependence of the vibration frequencies, are negligible for materials investigated here. Alternatively, it is, also, possible to estimate the elastic stiffness coefficients from numerical estimate as<sup>15</sup>:

$$C_{ij} = \frac{d^2 U}{d\varepsilon_i d\varepsilon_j} \quad (4)$$

where  $U$  is the potential energy of the system. Generally, it is assumed that the numerical estimation of second derivatives (of the energy) will be less precise than estimation of the first derivatives (of the stress). Therefore, the latter method has been used here for calculating the elastic constants. This approach creates the foundation of calculating elastic constants

Although the elastic stiffness coefficients could be obtained by estimating the second derivatives of the deformation energy with respect to strain using a finite difference formula (for diagonal components only), generally, the numerical approximation of second derivatives (of the energy) will be less precise than estimation of the first derivatives (of the stress). Therefore, the second part of (4) is used here for calculating the elastic constants.

The stress tensor<sup>15</sup> can be obtained using the following expression:

$$\sigma = -\frac{1}{V_0} \left[ \left( \sum_{i=1}^N m_i (v_i v_i^T) \right) + \left( \sum_{i<j} r_{ij} f_{ij}^T \right) \right] \quad (5)$$

where the index  $i$  denotes the particles,  $m_i$ ,  $v_i$  and  $f_i$  are the mass, velocity and force acting on particle  $i$ ; and  $V_0$  denotes the (undeformed) system volume. In an atomistic calculation, this expression for internal stress tensor is called virial expression.

As discussed before the MD simulations rely on chosen forcefield. In this paper, we mainly used Condensed-phase Optimized Molecular Potentials for Atomistic Simulation Studies (COMPASS) forcefield. This forcefield was chosen because it enables an accurate and simultaneous prediction of structural, conformational, vibrational and thermophysical properties for a broad range of molecules, in isolated and condensed phases, and under a wide range of temperature and pressure conditions. Different ensembles were applied for the different dynamic thermostat or barostat steps, such as NVT (constant-volume/constant-temperature) and NPT (constant-pressure/constant-temperature) dynamics.

The equations of motion were solved with the Anderson velocity algorithm for the NVT, and the Berendsen velocity algorithm for the NPT. The time step of integration was set to 1 fs (femto second) in all cases, which is the recommended time step for the type of atoms considered. The summation methods for van der Waals and Coulomb forces were all atom-based with a cutoff (spline and buffer) width of 9.5Å.

The Discover module within Materials Studio Software was used. Discover provides several methods for controlling temperature and pressure. Depending on which state variables (for example, energy  $E$ , volume  $V$ , temperature  $T$ , pressure  $P$ , and number of particles  $N$ ) are fixed, different statistical ensembles can be generated. A variety of properties, such as structural, energetic, and dynamic properties, can then be calculated from the averages or the fluctuations of

these quantities over the ensemble generated. Examples of stiffness matrices obtained using MD simulation are shown in the appendix of this paper.

### 3. GEOMETRICAL PARAMETERS

#### 3.1 Effect of MWCNT Building Method

The building a MWCNT structure is usually done by either maintaining a constant chiral innermost tube and then progressively adding the outer tubes (set 1), or by fixing the outermost tube and then adding the inner tubes (set 2). Previous studies showed that for the set 1 construction, elastic modulus increases with the increase of number of walls. For set 2 construction, elastic modulus and Poisson's ratio decrease with the increase of number of walls.<sup>7</sup>

Two methods were used to build the MWCNTs: sequential and individual. In the sequential method, the number of walls, chirality of innermost tube, minimum separation distance between CNTs, and the length of CNT were specified. The chirality of the outer walls is not assigned. The software automatically calculates the chirality of the outer walls one layer at a time by fixing the  $n$  vector and increasing  $m$  vector. According to Sears *et al.*,<sup>5</sup> the energetically favorable separation wall distance 3.4 Å; so in this study, the minimum separation distance was set to the thickness of a graphene sheet (3.347 Å), and an innermost chiral vector was fixed to be (5, 5).

In the individual method, the chirality of each wall of the MWCNT was specified. In this paper we simulated MWCNTs with chiral vectors of  $(5 \times n, 5 \times n)$ ,  $n = 1, 2, 3, \dots$ . This sequence is one of the most likely buildups for multi-walled tubes, because its interwall distance is very close to that observed experimentally.<sup>15,17</sup> In this paper we mainly focused on monochiral MWCNTs, because mixed chiral nanotubes with incommensurate periods along their axis will lead to a non-periodic system, which violates the Bloch theorem,<sup>18, 19,20</sup> thus making calculations more difficult.<sup>21</sup>

Typical stiffness matrices for MWCNT obtained using NPT thermodynamic ensemble and Berendsen (thermostat, barostat) velocity algorithm are shown below for the case of four walls:

$$C_{ij} = \begin{bmatrix} 202 & 21.6 & 11.2 & 0 & 0 & 0 \\ 15.9 & 45.5 & 11.9 & 0 & 0 & 0 \\ 21.7 & 36.9 & 23.7 & 0 & 0 & 0 \\ 0 & 0 & 0 & 3.2 & 0 & 0 \\ 0 & 0 & 0 & 0 & 10.41 & 0 \\ 0 & 0 & 0 & 0 & 0 & 1 \end{bmatrix} \text{GPa} \quad C_{ij} = \begin{bmatrix} 280 & 36.1 & 44.77 & 0 & 0 & 0 \\ 18.5 & 67.1 & 66.6 & 0 & 0 & 0 \\ 50.42 & 49.1 & 47.4 & 0 & 0 & 0 \\ 0 & 0 & 0 & 3 & 0 & 0 \\ 0 & 0 & 0 & 0 & 7.4 & 0 \\ 0 & 0 & 0 & 0 & 0 & 5.5 \end{bmatrix} \text{GPa}$$

*Sequential Simulation*

*Individual Simulation*

Shen and Li<sup>22</sup> reported analytical expressions for five independent effective elastic moduli of MWCNTs subjected to the axial tension, compression stresses, torsional moment, in-plane biaxial tension, and in-plane shear loadings, at small strain conditions. These expressions involve interwall elastic constants, which are used to describe the linear elastic relations between the interwall stresses and strains corresponding to the three basic interwall deformation modes. Examining the above matrices, one can conclude that the MWCNTs are transversely isotropic. Therefore engineering constants are calculated using the following relations<sup>23</sup>:

$$E_{11} = \frac{C_{11} - 2C_{12}^2}{C_{22} + C_{23}} \quad (6. a)$$

$$E_{22} = \frac{C_{22} + C_{12}^2(-C_{22} + C_{23}) + C_{23}(-C_{11} + C_{23} + C_{12}^2)}{(C_{11} * C_{22} - C_{12}^2)} \quad (6. b)$$

$$\nu_{12} = \frac{C_{12}}{C_{22} + C_{23}} \quad (6. c)$$

$$K_{23} = 0.5(C_{22} + C_{23}) \quad (6. d)$$

$$M_{23} = 0.5(C_{22} - C_{23}) \quad (6. e)$$

Figure 2 shows a plot of MWCNT's longitudinal elastic constant,  $E_{11}$ , for both building setups, sequential and individual, for the case of NPT thermodynamic ensemble. The result shows that different building ensemble has a minor effect on the calculated elastic constants.

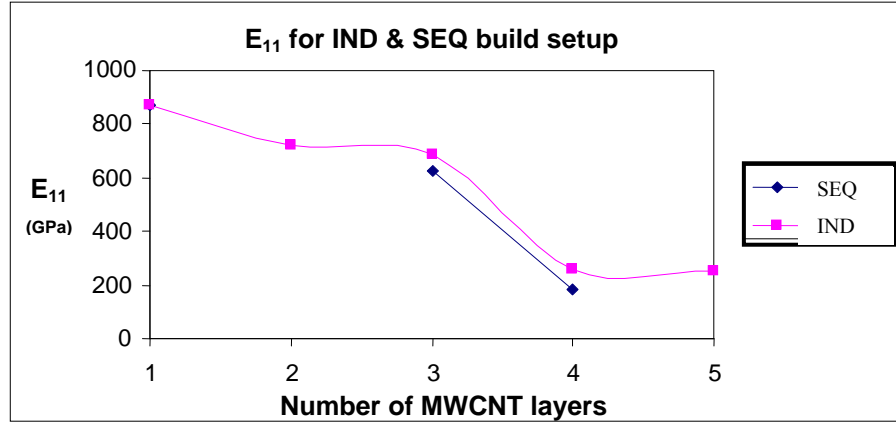


**Figure 2.** Longitudinal modulus,  $E_{11}$ , versus number of CNT layers using NPT ensemble for both sequential (SEQ) and individual (IND) setups.

### 3.2 Effect of Number of Layers

MWCNTs consist of several coaxial tubes, with outer diameter of 1.4 ~ 100 nm. Number of walls ranges from two to tens.<sup>24</sup> Thus, the second geometric parameter studied is the number of CNT layers (Figure 3).

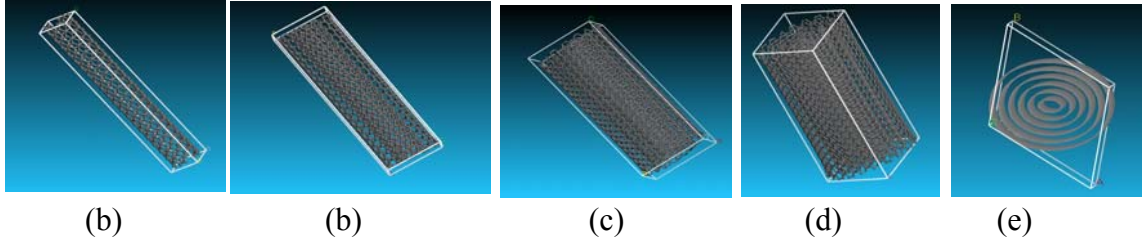


**Figure 3.** MWCNTs with chiral angle of  $(5*n, 5*n)$  for the cases of (a) SWCNT, 400 atoms, (b) DWCNT, 1200 atoms, (c) Three-walled CNT, 2400 atoms, (d) Four-walled CNT, 6000 atoms, and (e) Five-walled CNT, 12000 atoms.

Figure 4 shows longitudinal stiffness versus the number of layers for NPT (constant Number of particles, constant Pressure and constant Temperature) ensemble. It is observed that the SWCNT has the highest elastic longitudinal constant  $E_{11}$ . Increasing the number of layers results in a drop of mechanical properties. However, the modulus approaches a constant value after three layers. Therefore, three layers had been chosen as the optimum number of layers for simulation purposes in this study.

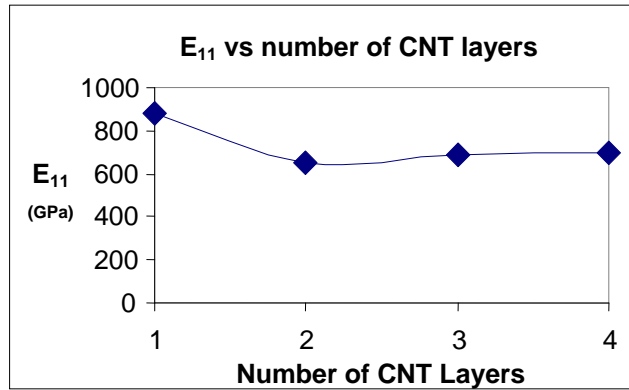


**Figure 4.** Longitudinal stiffness versus number of layers.

### 3.3 Effect of Super Cell Size

The unit cell is regarded as the basic “building block” of a crystal. It is an artificial cell used to represent the size, shape, and number of objects contained within a crystal. It is generally a parallelepiped defined by certain lattice parameters. These parameters are based on the characteristic angles and magnified distances of a crystal. The CNT unit cell block is a triclinic unit cell with  $\gamma=\beta=90^\circ$ ,  $\alpha=120^\circ$  (see Figure 5). The chirality and diameter of CNT define the length parameters  $B$  and  $C$  in Figure 5. The value of  $A$  defines the simulated length of the CNT.

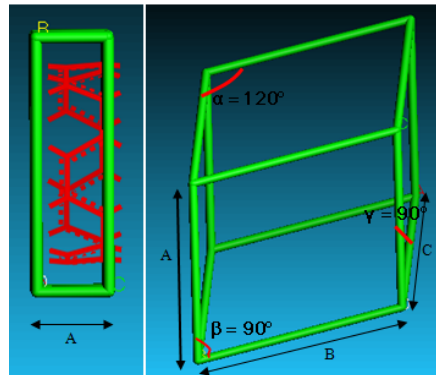


**Figure 5.** Schematic triclinic unit cell showing lattice parameters.

A super cell is constructed by repeating unit blocks in any of the symmetry axes. In order to simulate an infinite length, periodic boundary conditions (periodic cell) is usually used. A limitation of a periodic cell is that it is not possible to achieve fluctuations that have a wave

length greater than the length of the unit cell. The range of interactions is also important. If the cell size is large compared to the range, over which interactions act, there should be no problem. For example, for the relatively short range Lennard-Jones potential, the cell should have a side greater than  $6\sigma$  (where  $\sigma$  is the depth of potential well), which corresponds to about  $20.4 \text{ \AA}$  for carbon.<sup>25, 26, 27</sup> For longer range electrostatic interactions, the situation is more complicated; and long-range order interactions such as Columbic and dipolar need to be imposed upon the system and their potentials should be considered.

The effects of imposing a periodic boundary can be evaluated empirically by comparing results obtained using a variety of cell shapes and sizes.<sup>28</sup> The limitations of molecular modeling include not only the size of the unit cell, but also the time required to equilibrate the unit cell for energy interaction calculations between atoms. Several cell sizes for MWCNTs were considered to study the effect on engineering constants (Figure 6).

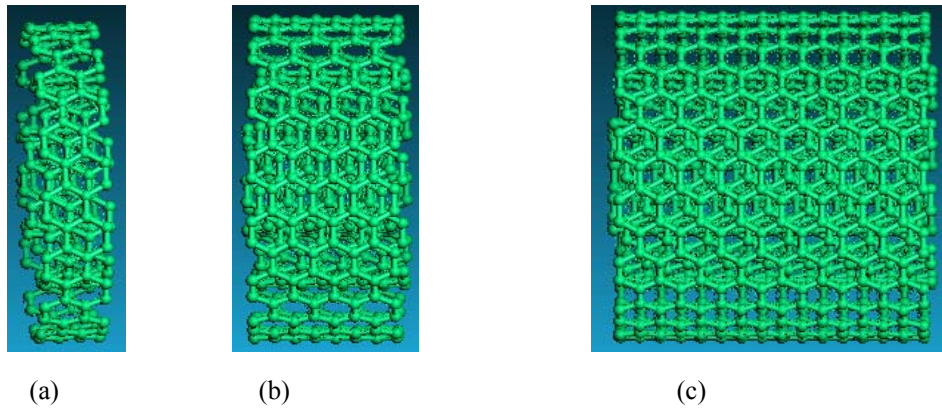


**Figure 6.** Typical simulated MWCNT for (a) two, (b) four, and (c) eight unit cells with assigned chirality vector  $(5, 5)$ ,  $(10, 10)$ ,  $(15, 15)$ .

Typical stiffness matrices for eight- and twenty-unit cell MWCNTs are given below:

- Eight unit super cell:

$$C_{ij} = \begin{bmatrix} 606.5 & 31.1 & 29.6 & 0 & 0 & 0 \\ 31 & 68 & 50.2 & 0 & 0 & 0 \\ 29.6 & 50.2 & 67.4 & 0 & 0 & 0 \\ 0 & 0 & 0 & .8 & 0 & 0 \\ 0 & 0 & 0 & 0 & .7 & 0 \\ 0 & 0 & 0 & 0 & 0 & 9.2 \end{bmatrix} GPa$$

- Twenty unit super cell:

$$C_{ij} = \begin{bmatrix} 698.1 & 25 & 25 & 0 & 0 & 0 \\ 25 & 66.2 & 49 & 0 & 0 & 0 \\ 25 & 49 & 66.4 & 0 & 0 & 0 \\ 0 & 0 & 0 & .8 & 0 & 0 \\ 0 & 0 & 0 & 0 & .6 & 0 \\ 0 & 0 & 0 & 0 & 0 & 8.6 \end{bmatrix} GPa$$

All simulations were performed under NPT ensemble (barostat: Berendsen; thermostat: Parrinello), where the boundaries of the unit cell were set to be free to allow for volumetric change during dynamic loading. The unit cell temperature was raised from 298°K to 400°K, and then cooled back to room temperature. Same procedure was applied for all the cases shown in Table 1. Different dynamic time was used for equilibrating the system at a rate of 1 fs per dynamic step. The total dynamic time is proportional to the total number of atoms (proportional to the length of CNT). From Table 1, it is reasonable to assume that, for this study case, 20 Å CNT is an optimal simulation length, because engineering properties are approaching constant values beyond that length.

**Table 1.** Engineering constants versus aspect ratio of a MWCNT.

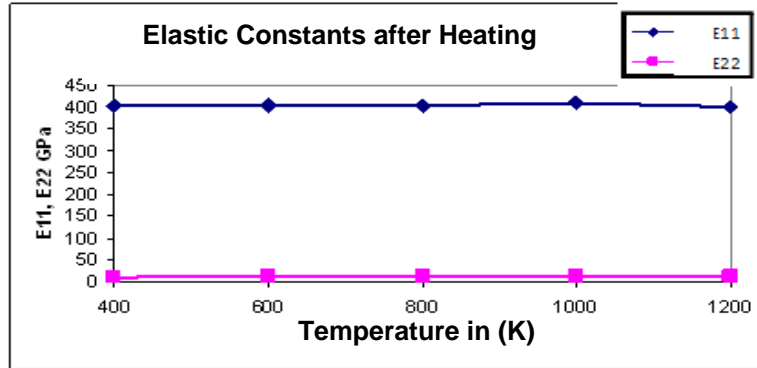
Three Wall	Length Å	$L/d$ Ratio Innermost	$L/d$ Ratio Outermost	$E_{11}$	$E_{22}$	$\nu_{12}$	$G_{23}$	$K_{23}$
2 units	4.92	0.72	0.25	439	36	0.20	11	47.3
4 units	9.84	1.5	0.50	493	36	0.26	7.7	47.15
8 units	20	3.63	1.20	590	31.1	0.26	9.0	59.2
20 units	49.2	7.3	2.40	687	30.0	0.26	8.6	57.6
30 units	73.8	11.0	3.60	690	27.5	0.33	7.9	52.6
40 units	98.4	14.4	4.80	720	28.6	0.33	8.3	54.9

## 4. SIMULATION PARAMETERS

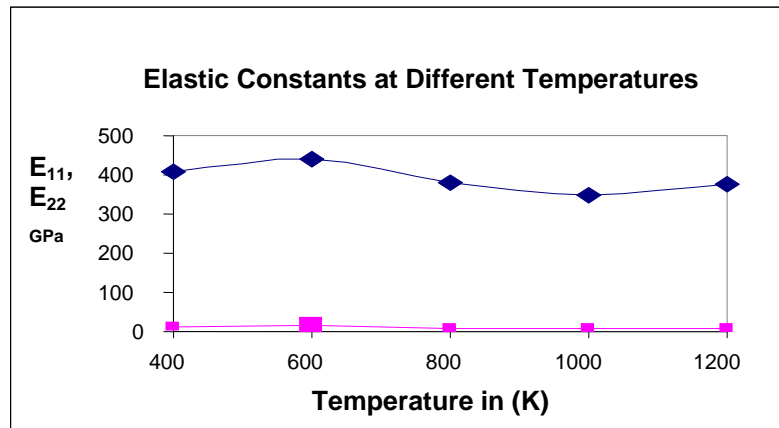
### 4.1 Heat Effect

CNTs can be created using arc discharge,<sup>29, 30, 31</sup> laser vaporization,<sup>32,33</sup> or catalytic decomposition of hydrocarbons.<sup>34</sup> Jacques *et al.*<sup>35</sup> demonstrated that high purity MWCNTs can be produced in bulk quantities on quartz substrates from a catalytic decomposition of a ferrocene-xylene mixture at 937°K.<sup>36, 37, 38</sup> Since CNTs are produced at high temperatures, a three-walled MWCNT was exposed to target temperatures of 400°, 600°, 800°, 1000°, and 1200°K. Two simulation sets were considered. In the first set, the temperature of MWCNT was raised from room temperature to target temperature and then cooled back to room temperature, at which elastic constants were calculated (see Figure 7(a)). In the second set, the temperature was

raised to target temperature, and elastic constants were calculated at that temperature (see Figure 7(b)). Figures 7(a), and 7(b) show that the elastic properties of MWCNTs are not affected by temperature scheme.



(a)



(b)

**Figure 7.** Elastic constants  $E_{11}$  &  $E_{22}$  of three-walled CNT for the case of (a) heated to different target temperatures and then cooled back to room temperature, and (b) heated to different target temperatures (NVT, Berendsen thermostat).

#### 4.2 Thermodynamics Ensemble Effect

The thermodynamic ensembles used in this study are:

##### a. Isothermal-Isobaric

This ensemble represents constant Number of atoms, constant Pressure, and constant Temperature (NPT). Therefore, NPT ensemble allows control of both temperature and pressure

with no new atoms entering the simulation cell. Free surface unit vector are allowed to change, and the pressure is adjusted by adjusting the volume. Energy fluctuation requires the use of a stochastic model for both forces and kinetic energy acting on the system of atoms. This process will average properties along the trajectories of pressure temperature, energy, volume cell parameters and stress so that it becomes equal to the NVT ensemble. Momentum will be affected instantaneously by the stochastic collision. The state of the system between collisions evolves according to Hamiltonian motion equations. Before performing simulation, temperature, mean rate of collision, and time at which particles collide are predetermined. Time at which particles suffer collision can be determined using a random number generator that follows Poisson distribution. Each collision changes the particle momentum to a new value chosen from a Boltzmann distribution. Finally, calculated trajectories of scaled systems are converted to the original system for the calculation of the time averages of any function,  $\bar{F}$ :<sup>11</sup>

$$\bar{F} = \lim_{T \rightarrow \infty} T^{-1} \int_0^T F(r^N(t), p^N(t); V(t)) dt \quad (7)$$

where  $F(r^N(t), p^N(t); V(t))$  is the mechanical state of the system at  $t \geq 0$ .

In a typical MD simulation,  $N$  and  $V$  are fixed, the initial choice for  $r^N(0), p^N(0)$  is made, and Hamilton's equation are solved numerically. Trajectory averages are then performed on the thermodynamic properties. The energy is conserved along the trajectory, and it is assumed that the trajectory spends equal times in all equal volumes with the same value of energy. It follows that:<sup>11</sup>

$$\bar{F} = F_{NVE}(N, V, E) \quad (8)$$

## **b. Isochoric**

This ensemble represents constant Number of atoms, constant Volume, and constant Temperature (NVT). It is also referred to as the canonical. The ensemble is obtained by controlling the temperature through direct temperature scaling during the initialization stage, and by temperature bath coupling during the data collection phase. The volume was kept constant through the run. This is the appropriate choice when conformational searches of molecules are carried out in a vacuum without periodic boundary defined. Even if periodic boundary conditions are used, and pressure is not a significant factor, the constant temperature and constant volume condition provides the advantage of less perturbation of the trajectory due to the absence of

coupling to a pressure bath. For the NVT ensemble, the velocities of the atoms,  $v_i$ , are rescaled by introducing an additional degree of freedom,  $s$ , which represents the external system. External and physical systems are both related through the expression:

$$v_i = s\dot{r}_i \quad (9)$$

This relation could be considered as the exchange of heat between both systems. Potential energy is associated with the degree of freedom  $s$  by  $(f+1)kT_{eq}$ , where  $f$  is the number of degree of freedom in the physical system,  $k$  Boltzmann's constant,  $T_{eq}$  is the externally set temperature.

The Lagrangian of the extended system of particles and  $s$  is thus postulated to be

$$\mathcal{L} = \sum_i \frac{m_i}{2} s^2 \dot{r}_i^2 - \phi(r) + \frac{Q}{2} \dot{s}^2 - (f+1)kT_{eq} \ln s \quad (10)$$

where  $\frac{Q}{2} \dot{s}^2$  is a kinetic energy term introduced to take into account a dynamic equation of  $s$ ,  $Q$  determines the time scale of temperature fluctuation, and  $\phi(r)$  is potential energy. For detailed derivations, refer to Refs. 39 and 40.

Figure 8 shows the longitudinal elastic constant versus the number of CNT walls for fixed super cells length. The drop in modulus in cases of four and five walls is the consequence of using a periodic cell of limited size; this result is different from the results shown in Figure 4 which are for a larger unit cell. The Figure 8 shows that the effect for the thermodynamic ensembles is relatively small.

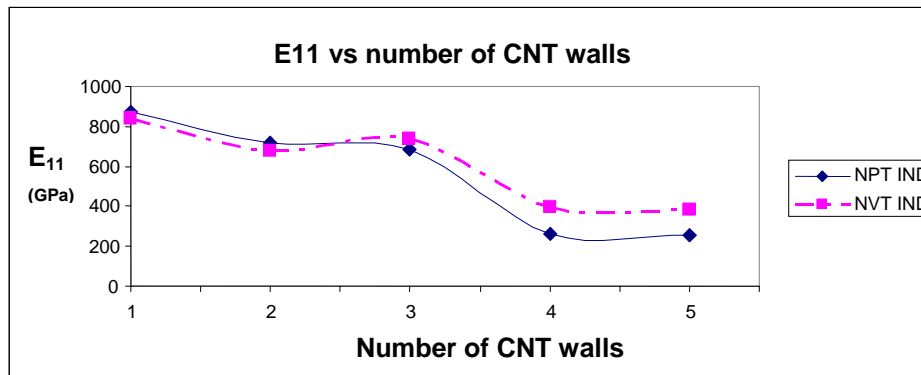


**Figure 8.**  $E_{11}$  versus number of layers, for NPT and NVT ensembles for a twenty-cell super cell.

### 4.3 Thermostat and Barostat Algorithms Effect

The following algorithms were used:

### **a. Berendsen algorithm**

This algorithm is used as a thermostat and a barostat dynamic control. The canonical ensemble does not allow temperature fluctuation. Berendsen thermostat allows the temperature of the system to be coupled to an external heat bath at a fixed temperature  $T_0$ . In this case the instantaneous temperature is pushed towards desired temperature by scaling velocities at each step. The momenta are increased or decreased towards the correct  $T$ . Temperature fluctuations will grow until trajectories are equivalent to NVE ensemble; however, they will never reach the canonical ensemble.

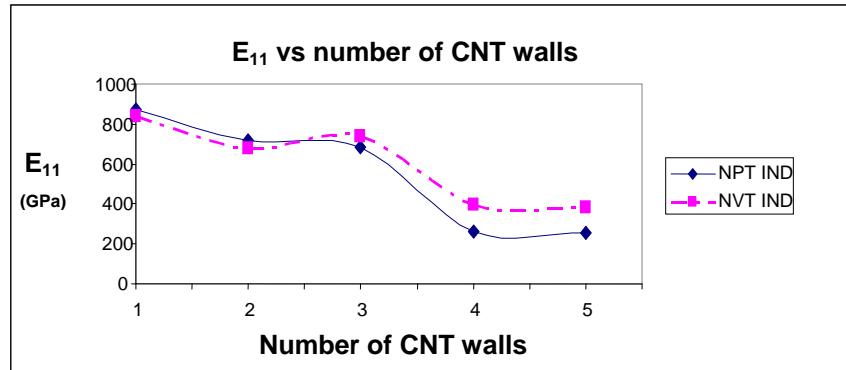
### **b. Andersen algorithm**

This thermostat algorithm is based on the stochastic collision of atoms, and it was the first thermostat algorithm proposed to simulate a canonical ensemble. For a particle suffered a collision, a new velocity is randomly assigned from a Maxwell-Boltzmann distribution at the desired temperature. The replacement is equivalent to a system being in contact with a heat bath that randomly emits thermal particles colliding with particles in the system, and changing their velocity. Between each collision, the system is simulated at constant energy. Thus, the overall effect is equivalent to a series of microcanonical simulations, each performed at a slightly different energy. The distribution of energies of these “mini-microcanonical” simulations should follow a Gaussian distribution. The Anderson thermostat generally yields good results for time independent properties.

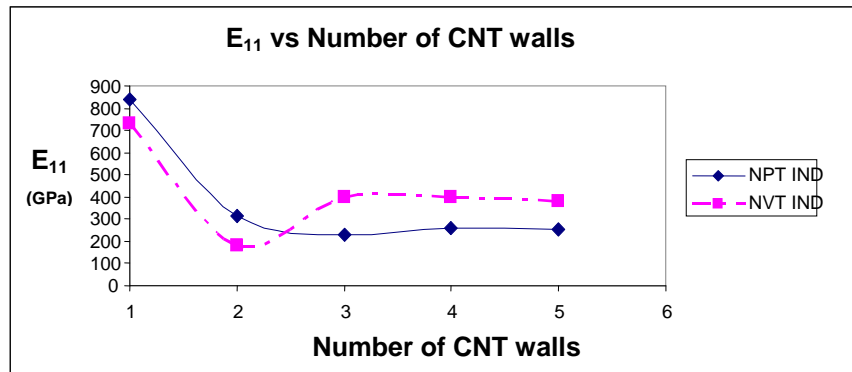
### **c. Parrinello algorithm**

Parrinello and Rahman<sup>39</sup> were the first to perform a generalized model for crystal structure MD simulations from Anderson constant pressure ensemble. Time dependent MD simulations allow volume and shape of crystals to vary with time.<sup>41</sup> This is a barostat algorithm, in which the induced dipoles are treated as additional dynamical variables that are included in the extended Lagrangian function. In the algorithm, mass is associated with the motion of dipoles. Given the starting configuration, the algorithm solves for the minimum energy of the electrons and evaluates the forces through energy derivatives with respect to nuclear positions. Figure 9 demonstrates the effect on elastic modulus by using different thermostat and barostat algorithms. For some of the cases, the difference is considerable. For example, for the case of DWCNT simulated under NVT ensemble, the longitudinal modulus is about 400 GPa for Berendsen

barostat and Berendsen Barostat, which is compared to about 750 GPa when Berendsen thermostat and Parrinello barostat are used.



(a) (Berendsen Thermostat and Parrinello Barostat)



(b) (Berendsen Thermostat and Berendsen Barostat)

**Figure 9.**  $E_{11}$  versus MWCNT layers.

## 5. CONCLUSIONS AND REMARKS

In this paper we investigated the various modeling issues involved in using molecular dynamics simulation for estimating the equivalent continuum mechanics elastic constants of multi-walled carbon nanotubes. These elastic constants are found to be sensitive to the carbon nanotube geometry (chirality, aspect ratio, number of walls) and the MD simulation conditions (temperature, thermodynamic ensemble, barostat and thermostat algorithms). From our analysis, we draw the following conclusions:

- Simulated mechanical properties of MWCNTs are sensitive to the aspect ratio of the super cell. Even by taking the advantage of periodic boundary condition, a super cell that

contains many periodic unit cells is required in order to obtain converged mechanical properties. The number of repeated units of a super cell also needs to increase with the increased number of CNT walls in order to maintain a proper aspect ratio of the super cell, as demonstrated in Table 1.

- The number of layers of a MWCNT poses a significant challenge for computer simulation time. Increasing the number of layers not only increases the number of atoms in each periodic unit cell, but also increases the number of unit cell required in a super cell. For example a periodic unit cell for a three-walled carbon nanotube contains 120 atoms. With a super cell of 8 unit cells, 960 atoms are required. For a four-walled CNT, 30 unit cells are generally required, leading to 6000 atoms.
- From Figure 4, which shows simulated result of CNT with different number of walls, it is shown that longitudinal engineering constants tend to reach constant values after the three-walled CNT. This converging result may allow MWCNT to be simulated with fewer number of walls, leading to significant saving in CPU time.
- We also observe that the effect of temperature path of the simulation appears to be small. The mechanical properties seem to be dependent only on the final temperature state.
- MWCNT build setup, either by individual or sequential method, did not affect the elastic constants.
- The equilibrated periodic unit cells of MWCNT are not affected by the thermodynamic ensemble used to control dynamic loading.
- Thermostat and barostat algorithms are one of the critical coupling effects on obtained mechanical properties of MWCNT. It is very important to choose the right combined algorithms. NVT thermodynamic is recommended to be combined with an Anderson thermostat algorithm. For NPT thermodynamic ensemble, it is recommended to use the Berendsen barostat, coupled with Parrinello thermostat.
- Results obtained from various types of loadings applied to MWCNT show that MWCNTs behaves as an equivalent linear elastic material, and are transversely isotropic.

We believe that the specific findings reported in this paper, as well as the general conclusions drawn from the findings may assist in the future investigation of equivalent continuum mechanics properties for MWCNT, and perhaps other carbon based nano materials.

## ACKNOWLEDGMENT

This work reported herein is partially supported by the funding received under a subcontract from the Department of Homeland Security-sponsored Southeast Region Research Initiative (SERRI) at the Department of Energy's Oak Ridge National Laboratory, USA. The authors also wish to acknowledge the partial support for this research by ONR Grant# N00014-07-1-1010, Office of Naval Research, Solid Mechanics Program (Dr. Yapa D.S. Rajapakse, Program Manager).

## REFERENCES

1. Treacy, M.M.J.; Ebbesen, T.W.; Gibson, T.M. *Nature* **1996**,381, 680-687.
2. Salvetat, J.P.; Bonard, J.M.; Thomsom, N.H.; Kulik, A.J.; Farro, L.; Bennit, W.; Zuppiroli, L. *J. Appl. Phys. A* 1999, 69, 255-260.
3. Ruoff, R.S. et al. *C. R. Physique* **2003**, 4, 993–1008.
4. Li, C.; Chou, T.W. *Composites Science and Technology* **2003**, 63, 1517-1524.
5. Batra, R.C.; Sears, A. *International Journal of Solids and Structures* **2007**, 44, 7577-7596.
6. Al-Ostaz, A.; Pal G.; *J. Mater. Sci.*, **2008**, 43,164-173.
7. Zhang, Y. Y.; Wang, C. M.; Tan, V. B. C. *Journal of Applied Physics* **2008**,103, 053505.
8. Liu, M; Cowley, J.M. *Carbon* **1994**, 32,393.
9. White, C.T.; Robertson, D.H.; Mintmire, J.W. *Physical Review B* **1993**, 47, 9.
10. Frenkel S., *Understanding Molecular Simulation From Algorithms and Applications*, 2nd ed.; Academic Press: San Diego, 2002.
11. Anderson H.C. Molecular dynamics simulations at constant pressure and/or temperature.
12. Lifson, S.; Warashel, A. *J. Chem. Phys.* 1968, 49, 5116.
13. Burkert, U.; Allinger, N. L. *Molecular Mechanics*; Caserio, M. C.,Ed.; ACS Monograph 77; American Chemical Society: Washington, DC,1989.
14. Sun, H. J. *Phys. Chem. B* 1998, 102, 7338-7364.
15. MS Modeling 4.0 Online Help Manual, Accelrys Inc., 2005.
16. Theodorou, D. N.; Suter, U.W. American Chemical Society, 1986,19, 139-154.
17. Lu, J.P. *Phys. Rev. Letter* 1997, 79, 1297.

18. Johnson, S.G.; Joannopoulos, J.D. *Introduction to Photonic Crystals: Bloch's Theorem, Band Diagrams, and Gaps* **2003**.
19. Matherell, A. J.; Fisher, R.M. *Physica Status Solidi*, **2006**, 32, 2, 551-562.
20. Lu, T.; Miao, X.; Metcalf, H. *Physical Review A* **2005**, 71, 061405.
21. Lambin, Ph.; Meunier, V.; Rubio A. *Phys. Rev. B* **2000**, 62, 5135.
22. Shen, L.; Li; J. *Phys. Rev. B* **2004**, 69, 045414.
23. Christensen R. *Mechanics of Composite Materials*, Krieger Publishing Company; Malbar, Fl, 1991, pp74-78.
24. Rakov, E. G. *Russ. Chem. Rev.* **2001**, 70, 827-863.
25. Liu, Y.; Wang, Q. *Phys. Rev. B* **2005**, 72, 085420.
26. Jakubov, T. S.; Mainwaring, D. E. *Adsorption* **2008**.
27. Bengtzelius, U. *Phys. Rev. A* **1986**,34,5059.
28. Leach R. A., *Molecular Modelling Principles and Application*, 2nd ed.; Pearson Education EMA, 2001.
29. Keidar, M. *J. Phys. D: Appl. Phys.* **2007**, 40, 2388-2393.
30. Levchenko, I.; Ostrikov, K.; Keidar, M.; Xu, S. *Applied physics letter*, **2006**, 89, 033109.
31. Huang, Z.P.; Xu, J. W.; Ren, Z. F.; Wang, J.H.; . *Applied physics letter*, **1998**, 73, 8345.
32. Chhowalla, M.; Teo, K. B. K.; Ducati, C.; Rupesinghe, N. L.; Amaratunga, G. A. J.; Ferrari, A. C.; Roy D , Robertson, J.; and Milne, W. I. *J. Appl. Phys.***2001**, 90, 5308.
33. Iijima, S. *Nature*, **1991**, 354, 56.
34. Ostrikov, K. *Rev. Mod. Phys.*,**2005**, 77, 489.
35. Jacques, D.; Villain, S.; Rao, A. M.; Andrews, R. Derbyshire, F.; Dickey, E. C.; Qian, D. **2003**
36. Gao, H.; Wu, X. B.; Li, J. T.; Wu, G. T.; Lin, J. Y.; Wu, K.; Xu, D. S. *J. Appl. Phys.***2003**, 83, 3389.
37. Kong, J.; Franklin, N. R.; Zhou, C.; Chapline, M. G.; Peng, S.; Cho, K.; Dai, H. *Science*, **2000**, 287, 622.
38. Levchenko, I.; Ostrikov, K.; Keidar, M.; Xu, S.; *J. Appl. Phys.*, **2005**, 98, 064304.
39. Parrinello, M.; Rahman, H.; Vashishta, P. *Physical Review Letter*, **1983**,50,1073.

## APPENDIX: EXAMPLES OF STIFFNESS MATRICES

Stiffness matrices for both individual and sequential setups under isochoric, and isobaric dynamic loadings are summarized below (values of elastic constants are in GPa):

### A1. NPT, Individual

**Table A1.** Molecular dynamics simulation parameters for MWCNT

<i>System setup</i>	Individual, 49.2 Å length
MD ensemble	NPT
Temperature	400 K
Thermostat	Berendsen
Barostat	Parrinello
Time step	1 femto second (fs)
Energy Deviation	100 kcal/mol

Chirality: (5,5)

$$C_{ij} = \begin{bmatrix} 880.1 & 7.8 & 8.6 & 0 & 0 & 0 \\ 8.4 & 31.21 & 17 & 0 & 0 & 0 \\ 9.13 & 16.1 & 35.5 & 0 & 0 & 0 \\ 0 & 0 & 0 & .8 & 0 & 0 \\ 0 & 0 & 0 & 0 & 2.1 & 0 \\ 0 & 0 & 0 & 0 & 0 & 5.7 \end{bmatrix}$$

Chirality: (5,5), (10,10)

$$C_{ij} = \begin{bmatrix} 674.4 & 39.9 & 62.4 & 96.9 & 0 & 0 \\ 38.1 & 67.4 & 48.2 & 0 & 0 & 0 \\ 62.5 & 50.7 & 65.7 & 0 & 0 & 0 \\ 93.7 & 0 & 0 & 16.4 & 0 & 0 \\ 0 & 0 & 0 & 0 & 41.9 & 0 \\ 0 & 0 & 0 & 0 & 0 & 9.4 \end{bmatrix}$$

Chirality: (5,5), (10,10), (15,15)

$$C_{ij} = \begin{bmatrix} 698.1 & 25 & 25 & 0 & 0 & 0 \\ 25 & 66.2 & 49 & 0 & 0 & 0 \\ 25 & 49 & 66.4 & 0 & 0 & 0 \\ 0 & 0 & 0 & .8 & 0 & 0 \\ 0 & 0 & 0 & 0 & .6 & 0 \\ 0 & 0 & 0 & 0 & 0 & 8.6 \end{bmatrix}$$

Chirality: (5,5), (10,10), (15,15), (20,20),(25,25)

$$C_{ij} = \begin{bmatrix} 271 & 21 & 16.47 & 0 & 0 & 0 \\ 20.5 & 37.41 & 19.71 & 0 & 0 & 0 \\ 16.7 & 19.9 & 28.5 & 0 & 0 & 0 \\ 0 & 0 & 0 & 5.5 & 0 & 0 \\ 0 & 0 & 0 & 0 & 1.25 & 0 \\ 0 & 0 & 0 & 0 & 0 & 2.4 \end{bmatrix}$$

## A2. NPT, Sequential

**Table A2.** Molecular dynamics simulation parameters for MWCNT

System setup	Sequential , 49.2 Å length
MD ensemble	NPT
Temperature	400 K
Thermostat	Berendsen
Barostat	Parrinello
Time step	1 femto second (fs)
Periodic boundary condition	ON
Energy Deviation	100 kcal/mol

Chirality: (5,5), (10,10)

Chirality: (5,5), (10,10), (15,15)

$$C_{ij} = \begin{bmatrix} 391.6 & 136.3 & 63.4 & 0 & 0 & 63.7 \\ 132.9 & 62.5 & 38.4 & 0 & 0 & 17.8 \\ 62.2 & 40.7 & 37.5 & 5 & 5 & 17.8 \\ 0 & 0 & 0 & 112.6 & 66 & 6 \\ 0 & 0 & 0 & 67.8 & 39.6 & 0 \\ 64.7 & 17.6 & 6.8 & 0 & 0 & 12.5 \end{bmatrix} \quad C_{ij} = \begin{bmatrix} 732.2 & 55.5 & 46.6 & 164.2 & 0 & 0 \\ 55.6 & 30.3 & 27.1 & 6 & 0 & 0 \\ 46.1 & 27.1 & 28.8 & 4.3 & 0 & 0 \\ 164.2 & 6 & 4.3 & 38.3 & 0 & 0 \\ 0 & 0 & 0 & 0 & 29.5 & 6.5 \\ 0 & 0 & 0 & 0 & 6.5 & 2.6 \end{bmatrix}$$

## A3. NVT, Individual

**Table A3.** Molecular dynamics simulation parameters for MWCNT

System setup	Individual, 49.2 Å length
MD ensemble	NVT
Temperature	400 K
Thermostat	Berendsen
Barostat	Parrinello
Time step	1 femto second (fs)
Periodic boundary condition	ON
Energy Deviation	100 al/mol

Chirality: (5,5)

$$C_{ij} = \begin{bmatrix} 878.9 & 17.3 & 19.1 & 0 & 0 & 0 \\ 19 & 59.2 & 40.5 & 0 & 0 & 0 \\ 19.1 & 42.8 & 61.9 & 0 & 0 & 0 \\ 0 & 0 & 0 & 2.6 & 0 & 0 \\ 0 & 0 & 0 & 0 & 1.7 & 0 \\ 0 & 0 & 0 & 0 & 0 & 9.4 \end{bmatrix}$$

Chirality: (5,5), (10,10), (15,15)

$$C_{ij} = \begin{bmatrix} 638.5 & 63.8 & 26.5 & 0 & 0 & 5.7 \\ 63.0 & 64.0 & 47.3 & 0 & 0 & 0 \\ 25.8 & 47.2 & 64.9 & 6.0 & 0 & 0 \\ 0 & 0 & 0 & 39.5 & 6.4 & 0 \\ 0 & 0 & 0 & 6.4 & 1.05 & 1.3 \\ 5.6 & 0 & 0 & 0 & 1.5 & 8.4 \end{bmatrix}$$

Chirality of walls: (5,5),(10,10)

$$C_{ij} = \begin{bmatrix} 780.4 & 27 & 26.3 & 0 & 0 & 0 \\ 26.3 & 69 & 60.7 & 0 & 0 & 0 \\ 26.4 & 58 & 63.7 & 0 & 0 & 0 \\ 0 & 0 & 0 & 0.5 & 0 & 0 \\ 0 & 0 & 0 & 0 & 1.4 & 0 \\ 0 & 0 & 0 & 0 & 0 & 9.5 \end{bmatrix}$$

Chirality: (5,5), (10,10), (15,15), (20,20)

$$C_{ij} = \begin{bmatrix} 378 & 6.8 & 4.8 & 0 & 0 & 0 \\ 7.2 & 4 & 1.4 & 0 & 0 & 0 \\ 7.4 & 1.1 & 1.8 & 0 & 0 & 0 \\ 0 & 0 & 0 & 3.6 & 0 & 0 \\ 0 & 0 & 0 & 0 & 3.5 & 0 \\ 0 & 0 & 0 & 0 & 0 & .7 \end{bmatrix}$$

#### A4. NVT, Sequential

**Table A4.** Molecular dynamics simulation parameters for MWCNT

System setup	Sequential, 49.2 Å length
MD ensemble	NVT
Temperature	400 K
Thermostat	Berendsen
Barostat	Parrinello
Time step	1 femto second (fs)
Periodic boundary condition	ON
Energy Deviation	100 kcal/mol

Chirality: (5,5), (10,10)

$$C_{ij} = \begin{bmatrix} 890.5 & 4.3 & 4.2 & 0 & 0 & 0 \\ 4.3 & 7.3 & 4.5 & 0 & 0 & 0 \\ 4.2 & 4.5 & 7.7 & 0 & 0 & 0 \\ 0 & 0 & 0 & 10 & 0 & 0 \\ 0 & 0 & 0 & 0 & 9.5 & 0 \\ 0 & 0 & 0 & 0 & 0 & 1.3 \end{bmatrix}$$

Chirality: (5,5), (10,10), (15,15)

$$C_{ij} = \begin{bmatrix} 856.5 & 4 & 3 & 0 & 0 & 0 \\ 4 & 5.3 & 2.5 & 0 & 0 & 0 \\ 2.6 & 2.5 & 4 & 0 & 0 & 0 \\ 0 & 0 & 0 & 3.7 & 0 & 0 \\ 0 & 0 & 0 & 0 & 3.4 & 0 \\ 0 & 0 & 0 & 0 & 0 & 1.2 \end{bmatrix}$$